

Acoustic Poisson-like effect in periodic structures

Alexey S. Titovicha) and Andrew N. Norris

Mechanical and Aerospace Engineering, Rutgers University, Piscataway, New Jersey 08854, USA

(Received 26 October 2015; revised 17 February 2016; accepted 15 March 2016; published online 30 June 2016)

Redirection of acoustic energy by 90° is shown to be possible in an otherwise acoustically transparent sonic crystal. An unresponsive "deaf" antisymmetric mode is excited by matching Bragg scattering with a quadrupole scatterer resonance. The dynamic effect causes normal unidirectional wave motion to strongly couple to perpendicular motion, analogous to the quasi-static Poisson effect in solids. The Poisson-like effect is demonstrated using the first flexural resonance in cylindrical shells of elastic solids. Simulations for a finite array of acrylic shells that are impedance and index matched to water show dramatic acoustic energy redirection in an otherwise acoustically transparent medium.

© 2016 Acoustical Society of America. [http://dx.doi.org/10.1121/1.4950709]

[MRH] Pages: 3353–3356

I. INTRODUCTION AND BACKGROUND

A sonic crystal (SC) is a periodic array of scatterers in an acoustic medium such as water or air. SCs originated as the acoustic analog of the early photonic crystals of Yablonovitch1 and John,2 which exhibited opaqueness at certain frequencies. Wave motion in SCs is characterized by Bloch waves, which, by virtue of the structural periodicity, can be folded in the wave number domain into the smallest indivisible unit cell, the irreducible Brillouin zone (BZ).³ The resulting band diagrams completely describe the SC frequency response, including bandgaps (BGs) formed by Bragg scattering when the incident wavelength is close to the lattice constant. BGs may be interpreted as bands of frequencies associated with a single Bloch wavelength, 4 within which an incident wave decays exponentially through the SC. A complete BG exists when a plane wave at any angle of incidence cannot propagate. The bandwidth of the BG depends on the filling fraction, shape, symmetry, orientation, and the relative impedance and/or density of individual scatterers.

The elasticity of the scatterer usually cannot be ignored in water-based SCs, as compared with air, where most scatterers can be considered as rigid. This can be used to advantage, for instance, to match the impedance of water. If the scatterer is a circular metal shell, there exists a unique thickness at which the scatterer impedance matches to water,⁵ maximizing transmission through an array. The reason⁶ is that although the metal has both stiffness and density greater than water, the effective stiffness and density of the shell are proportional to the thickness-to-radius ratio h/a < 1 and, therefore, a unique value of h/a exists at which the product of stiffness and density equals the square of the acoustic impedance of water. By varying h/a, it is also possible to tune either the quasi-static bulk modulus of the shell or its effective density to those of water, but it is rarely possible to match both simultaneously with some material exceptions.⁶ However, it is possible to match both the density and bulk modulus by inserting an axisymmetric elastic substructure into the shell.^{6,7} Matching the bulk modulus removes the monopolar response, while the matched density eliminates dipole radiation, dramatically reducing the scattering at subwavelength frequencies. Such control of quasi-static shell properties facilitates the design of refraction-based lenses.^{5,6}

Elastic shells provide rich scattering properties, mainly due to their ability to support highly dispersive flexural waves (in-plane bending), which are the topic of this paper. Waves scattered from flexural resonances in a SC interact with the propagating Bloch waves forming what are called quasi-bandgaps in the band diagram, which can occur at sub-wavelength frequencies. If the flexural resonant frequency is tuned to fall inside the first BG, narrow asymmetric transmission peaks (Fano-like asymmetry according to Kosevich *et al.* appear due to coherent scattering. These narrow regions of transmission were used by Khelif *et al.* to create a narrow passband filter, and later by Pennec *et al.* for demultiplexing an incident wave. Also, Kosevich *et al.* concluded that the BG bandwidth increases when a flexural resonance falls within it.

An important feature of SCs is the existence of antisymmetric (AS) bands, eigenmodes polarized in the direction perpendicular to the incident wave, as compared to symmetric (S) modes oriented along the incident direction. Sánchez-Pérez et al. 12 termed AS modes in a symmetrically insonified square array as deaf since their experiment was carried out in air at audible frequencies. They demonstrated that an AS mode is not excited by a normal plane wave onto an array of effectively rigid scatterers by comparing the experimental transmission data with the band diagram obtained with the plane wave expansion method. Later, Hsiao et al. 13 compared the band structure of steel circular cylinders in water obtained using the periodic-boundary finite element method, to the transmission simulations using the finite difference time domain method, as a way of separating out the deaf modes. Also, Laude et al. 17 demonstrated how AS modes are excited when the symmetry of the unit cell is not preserved.

Evanescent waves can play an important role in SCs. In a thorough analysis of the connection between propagating

a)Electronic mail: titovichalexey@gmail.com

and evanescent bands, Romero-Garcia *et al.*¹⁴ point out that the transfer of symmetry from one band to the other is via an evanescent mode. Similarly, repelled bands are connected by an evanescent band. These references emphasize that the deaf modes are coupled to the propagating mode at the boundaries of the BG, either in real or evanescent regions. However, Botey *et al.*¹⁵ recently showed for photonic crystals that one can "unlock" evanescent modes from the BZ boundaries resulting in evanescent beams escaping the photonic crystal. The beam forming is caused by the negative group velocity of the unlocked mode constituting negative refraction. The idea of utilizing evanescent modes is here extended to acoustics where the flexural mode of an elastic shell is the proposed mechanism for exciting an AS mode leading to perpendicular wave propagation.

The n=2 flexural mode is a constant volume mode (Fig. 1) that when excited by an incident wave transfers acoustic energy to a normal direction via the quadrupole scattering pattern. The displacement of this mode resembles the Poisson effect in solids, with conceptually similar repercussions, and is referred to as the acoustic Poisson-like effect. Generally, low order flexural modes are subsonic, scattering an evanescent wave that does not propagate into the far-field. However, in SCs where the lattice constant is on the order of the decay length of the evanescent wave, there is significant interaction between the incident wave and the flexural waves on adjacent shells. The orientation of the scattered quadrupole depends on the direction of incidence. In particular, a perpendicular wave front can emerge if the shells are spaced so that all scattered quadrupoles are in phase (i.e., when the spacing is close to the wavelength) at normal incidence. This is the central idea of this article.

II. ANALYSIS AND DISCUSSION

Consider a SC with square unit cell of side length b, containing an empty circular elastic shell of outer radius a, thickness h, density ρ_s , shear modulus μ_s , Poisson's ratio ν_s ,

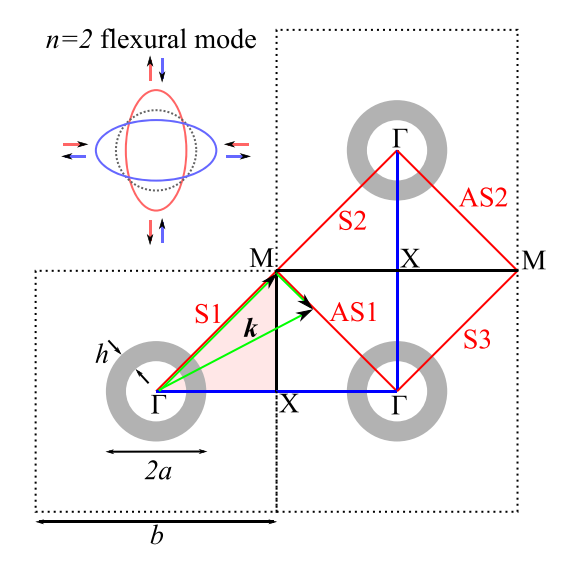


FIG. 1. (Color online) Square unit cells (dashed) consist of an empty shell in water. Overlaid on top are the first six irreducible BZs in reciprocal space, which have perimeters Γ XM. The n=2 flexural mode of an elastic shell is illustrated in the top left.

in water ($\rho = 1000 \text{ kg/m}^3$, K = 2.25 GPa), shown in Fig. 1. The material, radius, and thickness of the shell are selected such that: (i) the effective bulk modulus of the shell equals that of water $K_{\text{eff}} = K$, which eliminates the monopolar response, (ii) the effective density also matches, $\rho_{\rm eff} = \rho$, removing the sub-wavelength dipolar response and making the SC neutrally buoyant, and (iii) the n=2 flexural resonance is near 20 kHz, the designated frequency of interest (see Ref. 6 for tuning of quasi-static parameters). The shell's effective density is $\rho_{\rm eff} = \rho_s(h/a)(2-h/a)$ and the effective bulk modulus follows from plane strain elasticity as $K_{\rm eff} = \mu_s (2(1-\nu_s)\rho_s/\rho_{\rm eff}-1)^{-1}$. A thick acrylic shell $(a=1~{\rm cm},~h=0.62a)$ with density, Young's modulus and $\rho_s = 1190 \,\mathrm{kg/m^3}, \quad E_s = 2(1 + \nu_s) \mu_s$ Poisson's ratio = 3.2 GPa, ν_s = 0.35, satisfies these three criteria with n=2 flexural resonance at 15 678 Hz. The lattice constant b = 4.78 cm is selected so that the n = 2 resonance coincides with the first BG in the \(\Gamma X\) direction and corresponds to a low filling fraction of $f_s = 0.14$. There is no special reason for this choice of b other than minimizing the distance in frequency space from the n=2 resonance to the first ΓM BG while also minimizing the spacing between shells. The coherent scattering postulated in the previous paragraph is expected to occur near the first FM BG and also in the second ΓX BG.

Modes characterized by wave propagation in a perpendicular direction exist in any SC as AS modes. It is sufficient to look at a homogeneous square unit cell of water with artificial periodic boundary conditions to understand the origin and structure of AS modes. Figure 1 shows three adjacent unit cells, as well as the first six irreducible BZs of the square array. The first three symmetric BZ boundaries (labeled S1, S2, S3) correspond to propagation in the (1,1) direction and the first two AS BZ boundaries (labeled AS1, AS2) correspond to projected wave vectors in the (1,-1) direction.

Figure 2(a) shows the band diagram for the unit cell with the thick acrylic shell obtained using COMSOL (Burlington, MA). Plotted over the shell-water bands (shown with dots) are the bands for the water-only unit cell (dashed lines). These can be thought of as the fundamental or "starting" bands for any SC. They are obtained by equating the free space wave number $kb = 2\pi bf/c$ to the wave number shown in Fig. 1, and plotted as a function of the wave vector projection onto the BZ boundary. Defining the reduced wave vector as $\hat{k} = kb \in [0, \sqrt{2}\pi]$, the AS1 band can be expressed as $(2\pi bf/c)^2 = (\sqrt{2}\pi)^2 + (\hat{k})^2$, but because the bands are folded into $[0, \sqrt{2}\pi]$, the expression becomes $f = (c/2\pi b)(2\pi^2)$ $+(\sqrt{2}\pi-\hat{k})^2)^{1/2}$. Bands S1 and S2 are linear following $f = (c/2\pi b)\hat{k}$, whereas the AS2 band is $f = (c/2\pi b)(8\pi^2$ $+\hat{k}^2)^{1/2}$, and the S3 band is $f = (c/2\pi b)(2\pi^2 + (\sqrt{2}\pi b))$ $+\hat{k})^2$)^{1/2}. The remarkable proximity of the water-only bands with the shell-water bands is a consequence of tuning of the shell to the quasi-static properties of water, making the SC acoustically transparent and decreasing the BG width. It is important to note that the curvature of some bands is due to the artificial discretization of space by the triangular

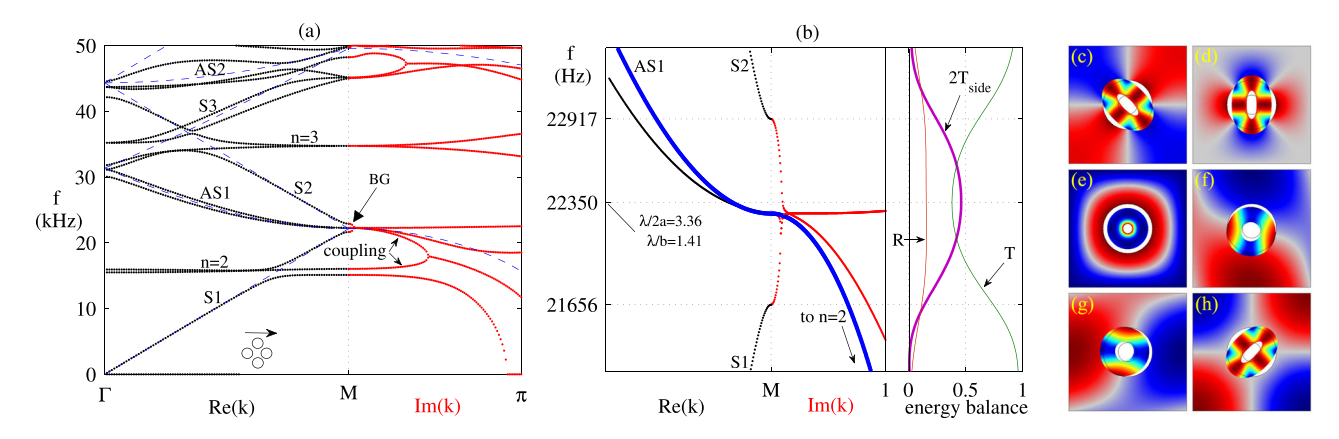


FIG. 2. (a) (Color online) Band diagram for unit cell with an acrylic shell along Γ M direction; the dashed lines are the bands for a water-only unit cell. (b) Magnified view of the first BG. The thick curve is the AS mode, which locks to the n=2 band. The three adjacent curves on the right show the fraction of the incident energy that goes out of the sides of a finite array $T_{\rm side}$, the back of the array T and the reflected energy R. The array is 8 shells deep in the direction of incidence and 41 shells wide. (c)–(h) First six modes along the line M in (a), corresponding to $\hat{k}=\sqrt{2}\pi$ in the (1,1) direction. The total pressure and displacement of the shell are shown, emphasizing the mode shapes. The frequencies in plots (c)–(h) are 15 123, 16 046, 21 656, 22 275, 22 275, and 22 917 Hz, respectively. The thick band in (b) at point M is mode (g), which locks to flexural mode (d).

irreducible BZ and the projection of the wave vector onto the boundary of an opposing BZ (see the *k* vector in Fig. 1).

Also shown are the evanescent bands, plotted by fixing the real value of $\hat{k} = \sqrt{2}\pi$. In order to excite the AS mode, the scatterer has to be non-axisymmetric, ¹⁷ breaking the geometrical symmetry of the unit cell. Another way to break the cell symmetry is with a non-axisymmetrically vibrating scatterer such as the n=2 flexural mode of a shell.

The band structure in Fig. 2(a) for the shell-water cell exhibits two pairs of flat bands caused by n=2 and n=3flexural modes of the shell. The two n=2 flexural modes near 16 kHz differ in their orientation, one is oriented with the corners and the other with the faces of the square unit cell [modes (c) and (d) in Fig. 2]. The former interferes with the S1 symmetric mode resulting in the veering of the bands. The flexural mode oriented with the faces is not directly excited, but rather couples to one of the AS1 modes via an evanescent band [pointed out with a pair of arrows in Fig. 2(a)]. The flexural mode represents a local resonance and is thus independent of the array periodicity. The coupling of a flexural mode to the AS1 band is what allows transfer of the incident wave energy to a perpendicular direction. A magnified view of the BG is shown in Fig. 2(b), where the excited AS1 band is displayed with a thick line and the other AS1 band locks to the lower BG boundary by an evanescent band. This effect differs from a near-zero-index material 16 that depends on the accidental degeneracy of modes at the center of the BZ (Γ point) where linear dispersion is key.

On the right of Fig. 2(b) is the energy balance for an array 8 cells deep by 41 cell wide insonified by a plane wave from the bottom (see array in Fig. 3). The transmission and reflection coefficients are obtained by integrating the intensity I over the four sides of the array yielding energy $E = \int I \cdot n \, dL$, and leading to definitions of the transmission from the side $T_{\text{side}} = E_{\text{left}}/E_{\text{inc}}$, transmission from the back $T = E_{\text{top}}/E_{\text{inc}}$, and reflection from the front $R = 1 - T - 2T_{\text{side}}$. The sideways transmission T_{side} is centered about the BG since it depends on the coherent scattering of shell-borne flexural waves, which occurs when the wavelength is

on the order of the lattice constant. Therefore, this acoustic Poisson-like effect is evident even for a mono-layer of shells, but strengthens with multiple layers. The peak sideways transmission for this array is 46% at 22 350 Hz. A simulation of a Gaussian beam incident onto the bottom of the array with a frequency of 22 350 Hz is shown in Fig. 3(a). The absolute pressure field shows very strong beams projecting symmetrically from the sides of the array. There is a pressure magnification at the sides of the array as compared to the incident wave, but this can be attributed to the aspect ratio of the array. Also shown in Fig. 3(b) is the same simulation, but at a higher frequency of 27 000 Hz, where the beam passes unabated through the array due to the tuning described earlier.

In comparison, Fig. 4 shows the band diagram for a rigid cylinder of the same radius and lattice constant along the Γ M direction. The AS1 bands are deaf and have the typical form for a SC of rigid scatterers. There is little agreement with the water-only bands (shown with the dashed lines) due to the effective impedance/index mismatch. However, the

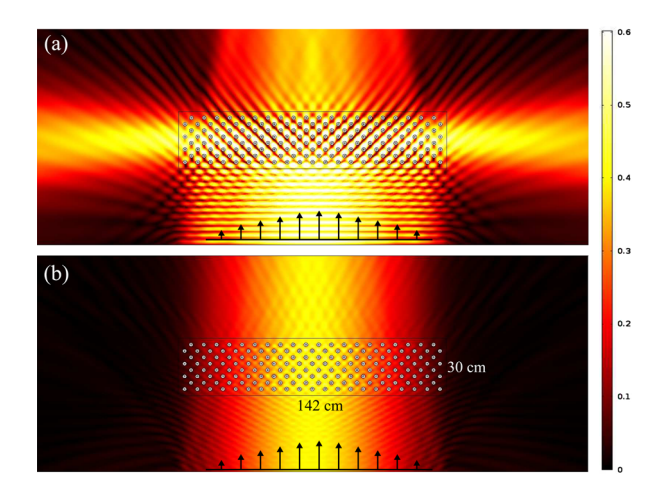


FIG. 3. (Color online) Absolute pressure field for a Gaussian beam incident upon an 8×41 array of acrylic shells in water. Plots (a) and (b) are at $22\,350\,\mathrm{Hz}$ and $27\,000\,\mathrm{Hz}$, respectively.

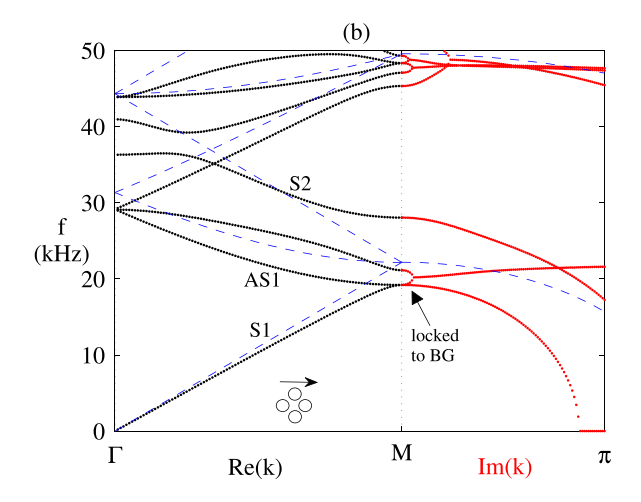


FIG. 4. (Color online) Band diagram for a unit cell with a rigid cylinder along ΓM direction.

BG bandwidth does increase dramatically by the same argument.

III. CONCLUSIONS

In conclusion, we present an effect in SCs, whereby a normally incident wave is passively and non-refractively transferred to a perpendicular direction. This acoustic Poisson-like effect is possible due to a non-axisymmetric local resonance in the form of the n=2 flexural mode of an elastic shell and an AS mode of the SC unit cell. We describe how this typically deaf mode is excited when it couples to the n=2 flexural mode. Simulations of a Gaussian beam onto a finite array of shells show that 46% of the incident energy is ejected from the sides of the array. It is conceivable that improved transmission from the sides of the array can be achieved by increasing the filling fraction and further decreasing the spacing between the first ΓM BG and the flexural mode. This Poisson-like effect is expected to occur in other crystals that can support similar n = 2 vibrations such as hollow/solid cylinders/spheres embedded in fluid or elastic materials, or even non-axisymmetric scatterers on plates for flexural waves. One could even envision this effect for electromagnetic waves in carbon nanotube (CNT) forests, since CNTs exhibit n = 2 vibrational modes. ¹⁸

ACKNOWLEDGMENTS

This work was supported by the Office of Naval Research (ONR) through Multidisciplinary University Research Initiatives (MURI) Grant No. N00014-13-1-0631

and Naval Undersea Research Program (NURP) Grant No. N00014-13-1-0417.

- ¹E. Yablonovitch, "Inhibited spontaneous emission in solid-state physics and electronics," Phys. Rev. Lett. **58**(20), 2059–2062 (1987).
- ²S. John, "Strong localization of photons in certain disordered dielectric superlattices," Phys. Rev. Lett. **58**(23), 2486–2489 (1987).
- ³L. Brillouin, *Wave Propagation in Periodic Structures* (Dover, New York, 1953).
- ⁴C. E. Bradley, "Acoustic Bloch wave propagation in a periodic wave-guide," Technical Report No. ARL-TR-91-19, Applied Research Laboratories at University of Texas at Austin, 1991.
- ⁵T. P. Martin, C. N. Layman, K. M. Moore, and G. J. Orris, "Elastic shells with high-contrast material properties as acoustic metamaterial components," Phys. Rev. B **85**(16), 161103 (2012).
- ⁶A. S. Titovich and A. N. Norris, "Tunable cylindrical shell as an element in acoustic metamaterial," J. Acoust. Soc. Am. 136(4), 1601–1609 (2014).
 ⁷A. S. Titovich and A. N. Norris, "Acoustic scattering from an infinitely long cylindrical shell with an internal mass attached by multiple axisymmetrically distributed stiffeners," J. Sound. Vib. 338, 134–153 (2015).
- ⁸Y. A. Kosevich, C. Goffaux, and J. Sánchez-Dehesa, "Fano-like resonance phenomena by flexural shell modes in sound transmission through two-dimensional periodic arrays of thin-walled hollow cylinders," Phys. Rev. B **74**(1), 012301 (2006).
- ⁹U. Fano, "Effects of configuration interaction on intensities and phase shifts," Phys. Rev. **124**(6), 1866–1878 (1961).
- ¹⁰A. Khelif, P. A. Deymier, B. Djafari-Rouhani, J. O. Vasseur, and L. Dobrzynski, "Two-dimensional phononic crystal with tunable narrow pass band: Application to a waveguide with selective frequency," J. Appl. Phys. 94(3), 1308–1311 (2003).
- ¹¹Y. Pennec, B. Djafari-Rouhani, J. O. Vasseur, A. Khelif, and P. A. Deymier, "Tunable filtering and demultiplexing in phononic crystals with hollow cylinders," Phys. Rev. E 69(4), 046608 (2004).
- ¹²J. V. Sánchez-Pérez, D. Caballero, R. Mártinez-Sala, C. Rubio, J. Sánchez-Dehesa, F. Meseguer, J. Llinares, and F. Gálvez, "Sound attenuation by a two-dimensional array of rigid cylinders," Phys. Rev. Lett. 80(24), 5325–5328 (1998).
- ¹³F.-L. Hsiao, A. Khelif, H. Moubchir, A. Choujaa, C.-C. Chen, and V. Laude, "Complete band gaps and deaf bands of triangular and honeycomb water-steel phononic crystals," J. Appl. Phys. 101, 044903 (2007).
- ¹⁴V. Romero-Garciá, J. O. Vasseur, L. M. Garcia-Raffi, and A.-C. Hladky-Hennion, "Theoretical and experimental evidence of level repulsion states and evanescent modes in sonic crystal stubbed waveguides," New J. Phys. 14, 023049 (2012).
- ¹⁵M. Botey, Y. Cheng, V. Romero-Garcia, R. Picó, R. Herrero, V. Sánchez-Morcillo, and K. Staliunas, "Unlocked evanescent waves in periodic structures," Opt. Lett. 38(11), 1890–1892 (2013).
- ¹⁶F. Liu, X. Huang, and C. T. Chan, "Dirac cones at k = 0 in acoustic crystals and zero refractive index acoustic materials," Appl. Phys. Lett. **100**, 071911 (2012).
- ¹⁷V. Laude, R. P. Moiseyenko, S. Benchabane, and N. F. Declercq, "Bloch wave deafness and modal conversion at a phononic crystal boundary," AIP Adv. 1, 041402 (2011).
- ¹⁸A. M. Rao, E. Richter, S. Bandow, B. Chase, P. C. Eklund, K. A. Williams, S. Fang, K. R. Subbaswamy, M. Menon, A. Thess, R. E. Smalley, G. Dresselhaus, and M. S. Dresselhaus, "Diameter-selective Raman scattering from vibrational modes in carbon nanotubes," Science 275(5297), 187–191 (1997).